ACS SyntheticBiology

pubs.acs.org/synthbio

Research Article

Engineering Alternate Ligand Recognition in the PurR Topology: A System of Novel Caffeine Biosensing Transcriptional Antirepressors

Ronald Rondon and Corey J. Wilson*

Cite This: *ACS Synth. Biol.* 2021, 10, 552–565

Read Online

ACCESS | Metrics & More | Article Recommendations | Supporting Information

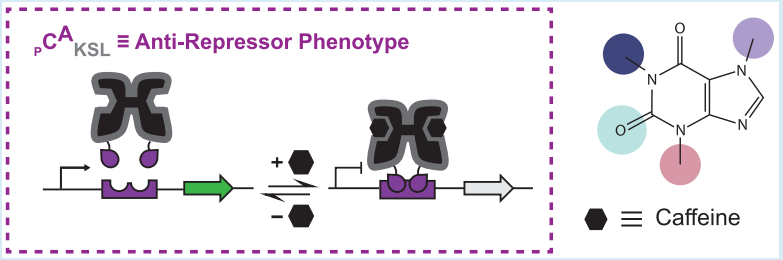

ABSTRACT: Recent advances in synthetic biology and protein engineering have increased the number of allosteric transcription factors used to regulate independent promoters. These developments represent an important increase in our biological computing capacity, which will enable us to construct more sophisticated genetic programs for a broad range of biological technologies. However, the majority of these transcription factors are represented by the repressor phenotype (BUFFER), and require layered inversion to confer the antithetical logical function (NOT), requiring additional biological resources. Moreover, these engineered transcription factors typically utilize native ligand binding functions paired with alternate DNA binding functions. In this study, we have advanced the state-of-the-art by engineering and redesigning the PurR topology (a native antirepressor) to be responsive to caffeine, while mitigating responsiveness to the native ligand hypoxanthine—*i.e.*, a deamination product of the input molecule adenine. Importantly, the resulting caffeine responsive transcription factors are not antagonized by the native ligand hypoxanthine. In addition, we conferred alternate DNA binding to the caffeine antirepressors, and to the PurR scaffold, creating 38 new transcription factors that are congruent with our current transcriptional programming structure. Finally, we leveraged this system of transcription factors to create integrated NOR logic and related feedback operations. This study represents the first example of a system of transcription factors (antirepressors) in which both the ligand binding site and the DNA binding functions were successfully engineered in tandem.

KEYWORDS: *engineered system of transcription factors, synthetic biology, gene regulatory network: protein engineering*

Synthetic biology is a rapidly evolving discipline[1] that draws upon fundamentals of biology and engineering[2] to rationally construct sophisticated gene circuits, which have recently come to the forefront of biomedical research. Through countless design−build−test cycles,[3] scientists have pieced together well-characterized biological modules to bring about complex cellular behaviors, enabling advances in personalized medicine,[4,5] biosensors,[6−8] and diagnostics.[9−11] The crux of these technologies is the precise control over gene expression, which is essential for the functionality of synthetic gene circuits. This becomes especially relevant in cell-based therapies, where precise gene expression is used to regulate the dosage of the produced therapeutic, thus enabling dynamic control of the behavior of cellular systems. Broadly speaking, gene expression in genetic circuits can be controlled either at the transcriptional or the translational level. While many recent advances have been made in controlling gene expression at the translational level using ribozymes or riboswitches,[12] most genetic circuits act at the transcriptional level by regulating promoter activity through the use of allosteric transcription factors (TFs).[13] Transcription factors make up a particularly valuable class of genetic switches because they are prevalent throughout the prokaryotic kingdom.[14] Importantly, allosteric transcription factors have evolved to recognize a broad variety of chemical structures,[15] and often share a modular domain structure composed of a conserved DNA-binding domain (DBD) linked to a diversified regulatory core domain (RCD).[16,17] Several groups have leveraged this modular structure and adopted RCD-swapping strategies into platform DBDs to rationally engineer novel transcription factors for a

Received: November 17, 2020
Published: March 9, 2021

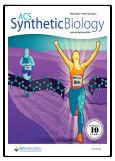

https://dx.doi.org/10.1021/acssynbio.0c00582
ACS Synth. Biol. 2021, 10, 552−565

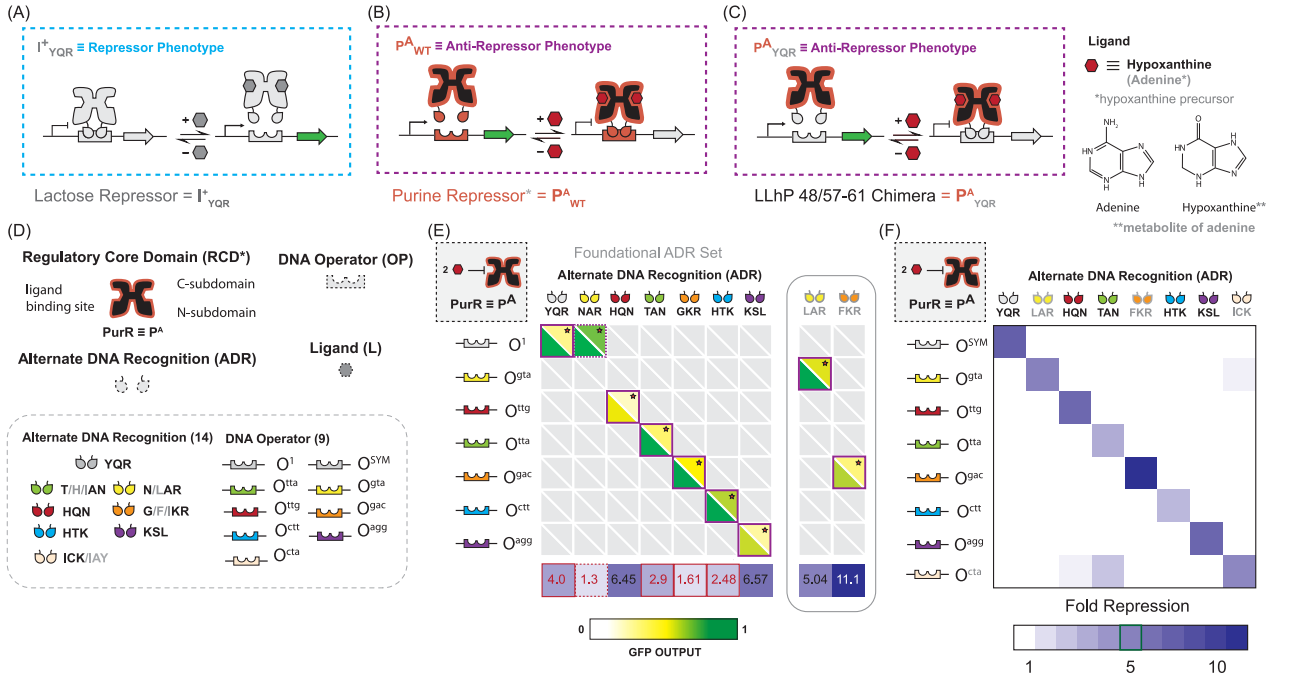

Figure 1. Modular design of the purine repressor (P^{A}_{YQR}) chimera. (A) The native phenotype for the lactose repressor, LacI (I^{+}). Gene expression is repressed in the absence of inducer by binding to the operator and induction is achieved upon addition of ligand *via* a conformational shift. (B) The *E. coli* purine repressor, PurR (P^{A}_{WT}), exhibits the antirepressor phenotype. In the absence of ligand, the protein is in the low DNA affinity state, allowing gene expression, while addition of ligand leads to diminished gene expression. (C) The previously reported LLhP 48/57−61 Chimera (P^{A}_{YQR}) consists of the regulatory core domain (RCD) from PurR and the DNA binding domain (DBD) of LacI, allowing for interaction with the O^{1} DNA operator while responding to the native ligand, hypoxanthine (adenine is metabolized into hypoxanthine *in vivo* and is used as the input signal). (D) The regulatory protein template. This system consists of a dimeric transcription factor (TF) along with its corresponding ligand (L), and its cognate DNA operator (OP). (E) Repression matrix for P^{A} with alternate DNA recognition. The bottom left triangle shows (OD_{600} normalized) GFP output in the absence of inducer, while the top right shows GFP output in the presence of 0.6 mM adenine. Red stars denote a statistically significant difference between the two states at $\alpha = 0.001$ level using a one-tailed Student's *t* test. Values correspond to the mean of $n = 6$ biological replicates. Values along the bottom of the matrix indicate the dynamic range for each variant (ratio between the "ON" and "OFF" states). The matrix on the left indicates our foundational ADR set indicating ADR-operator pairs from our previous work, while the two columns on the right represent new ADR units that will replace those with poor performance. Note: The bottom left triangles are dissimilar due to variation in promoter strength imposed by the operator and low affinity TF binding in the absence of ligand.[18] (F) Heatmap illustrating the dynamic range of each ADR-operator pairing using the same data. A dynamic range of approximately 5 was used as a reference, as that denotes the performance of the native lactose repressor. The ICK-O^{cta} pair has been added to expand our set of TF-operator pairs.

variety of applications.[18−23] Purportedly, the RCD manages the initial allosteric response in a given TF, which modulates DNA binding, as observed in the LacI system, see Figure 1A. Acknowledging that allosteric regulation relies on complex interdomain interactions,[24] the *de novo* (rational) design of an allosteric TF is currently intractable. However, scientists have successfully leveraged laboratory evolution strategies to engineer transcription factors with user-defined changes in small-molecule specificity,[25−27] desired changes in dynamic-operating ranges,[28] as well as inversion-of-function.[29−31] Many of these functions involve some aspect of allosteric communication.

The *Escherichia coli* (*E. coli*) purine repressor (PurR) is a member of the LacI/GalR family responsible for regulating expression of the genes involved in *de novo* purine nucleotide biosynthesis,[32] as well as several other genes having related functions in nucleotide biosynthesis and metabolism.[33−37] Of all the members of the LacI/GalR family, PurR has the highest sequence identity with lactose repressor (LacI), ∼32%,[38] and a similar tertiary structure has been confirmed by comparing the X-ray crystallographic structures of the two proteins.[39−41] Unlike most members of the LacI/GalR family (which naturally respond to small molecule sugars) PurR responds to the ligand hypoxanthine, functioning natively as an antirepressor (Figure 1B).[36] Purines—more specifically, xanthines—are an important class of bioactive and physiologically relevant molecules that can serve as both biomarkers of disease[42−44] as well as therapeutics.[45−49] Arguably the most notable xanthine,[50] caffeine (1,3,7-trimethylxanthine), is an ideal target for a trigger-inducible gene switch as it is relatively nontoxic,[51] cheap to produce, and only present in specific beverages, such as coffee and tea.[52] In previous work, most caffeine-responsive gene switches required the enzymatic conversion of caffeine to theophylline for translational control in yeast.[53] However, several caffeine biosensors have been developed in recent years,[54,55] although none are based on transcription factors, likely because existing caffeine-inducible TFs are rare and poorly characterized.[56] We posited that PurR could serve as a scaffold for engineering a caffeine responsive transcription factor given the similarity in chemical structure of the putative ligand (caffeine) to the native ligand (hypoxanthine). Moreover, since this particular class of TFs generally have a relatively simple mode of action and do not require additional biological components from the host, they can be used to regulate gene expression in a variety of different organisms.[57−60]

https://dx.doi.org/10.1021/acssynbio.0c00582
ACS Synth. Biol. 2021, 10, 552−565

In this work, we begin by equipping the LacI:PurR chimera LLhP 48/57−61[61] (Figure 1A−C) (henceforth referred to as P^A) with alternate DNA recognition (ADR) according to our previously established methodology. This workflow generated 7 additional TFs with orthogonal DNA binding ability and reinforces the notion that the LacI/GalR family is a rich resource that can be mined for the creation of novel chimeric TFs with shared DNA binding ability. Next, we used a combination of rational design and laboratory evolution to develop a system of caffeine responsive transcription factors with varying degrees of ligand sensitivity as well as dynamic operating ranges. Finally, the DNA binding domains of these caffeine responsive antirepressors were modularly altered to yield a collection of 30 novel TFs with mitigated response toward the natural ligand (hypoxanthine). This ability to completely abolish the response (including noninducible antagonism) toward the native ligand stands in stark contrast to other attempts to alter ligand specificity in similar scaffolds,[62−64] and is a direct result of our engineering workflow. These novel TFs respond to several other methylxanthines, allowing for the construction of logical NOR operations, which are crucial in genetic circuit design as they are functionally complete, and can be composed to implement any logic function.[65] This study represents the first example of a system of TFs (antirepressors) in which both the ligand binding site and the DNA binding functions were successfully engineered in tandem.

RESULTS

Part I: Building a System of Purine (PurR) Antirepressors with Alternate DNA Binding. The overarching goal of this study is to engineer a system of caffeine responsive antirepressors, that can work collaboratively within our transcriptional programming edifice. To accomplish this we first need to demonstrate that the parent PurR scaffold is amenable to ADR adaptation with our basis ADR set. In previous studies, we have demonstrated a modular protein design strategy to confer alternate DNA-binding functions in several repressor scaffolds that share a topology (*i.e.*, LacI, GalR, GalS, RbsR, FruR, and CelR).[18,20] Here we leverage our established modular design workflow to pair alternate DNA recognition (ADR) with the PurR regulatory core domain (RCD). In contrast to the aforementioned repressors, PurR natively functions as an antirepressor—*i.e.*, with a phenotype that is antithetical to LacI and related transcription factors (see Figure 1A,B). Tungtur *et al.* generated a PurR chimera P^A_{YQR} adapted with a wild-type LacI DNA binding domain (YQR) that retains the antirepressor function but interacts with the native LacI DNA operator (O^1) (Figure 1C).[61] The YQR nomenclature specifies the primary structure positions Y17, Q18, and R22, and are regarded as the principal residues that facilitate DNA binding. The "A" superscript denotes the antirepressor phenotype, in accordance with our previously reported designations.[29,31] We posited that the P^A_{YQR} chimera could serve as the basis for additional alternate DNA binding adaptation given that the YQR DBD was used as the reference domain for our previously reported ADR variants. Moreover, we surmised that the resulting system of PurR based transcription factors would function as antirepressors, interacting exclusively with cognate DNA binding elements.

Initially, the PurR regulatory core domain was adapted with our foundational alternate DNA binding domains NAR, HQN, TAN, GKR, HTK, and KSL. In turn, the six putative transcription factors were benchmarked against the cognate operators O^{gta}, O^{tta}, O^{gac}, O^{ctt}, and O^{agg}, respectively (Figure 1D,E). Including the $P^A_{YQR}|O^1$ basis set, this resulted in a putative system of seven antirepressor transcription factors responsive to hypoxanthine (*i.e.*, a metabolite of adenine). Here the design goal was based on two-criteria: (i) dynamic range on the cognate operator element, and (ii) orthogonal operator DNA binding. The gene regulator LacI (I^+_{YQR}) has been used in a myriad of genetic circuits across a variety of host organisms[57−60] and can therefore be regarded as a reference point in gauging the performance of engineered transcription factors. The standard LacI repressor system ($I^+_{YQR}|O^1$) performs with a dynamic range of approximately 5, according to our previous reports.[20,31] To this end, we compared the dynamic range of these engineered P^A_{ADR} with the wild type LacI system ($I^+_{YQR}|O^1$)—*via* regulating green florescent protein (GFP) output—positing that systems with similar (or better) performance metrics can be regarded as robust gene regulators. Initially, only two out of the seven transcription factor DNA pairs had a fold antirepression (dynamic range) greater than or equal to 5 while the $P^A_{YQR}|O^1$, $P^A_{NAR}|O^{gta}$, $P^A_{TAN}|O^{tta}$, $P^A_{GRK}|O^{gac}$, and $P^A_{HTK}|O^{ctt}$ systems had performance metrics below the $I^+_{YQR}|O^1$ reference system (Figure 1E).

To improve the performance of our transcription factors, while retaining modulated interaction with the foundational operators, we evaluated additional ADR variants that can interact with the existing operator set. Here we selected ADR variants from the combinatorial space generated by Milk *et al.*[66] In this study, Milk and colleagues generated over 8000 putative alternate DNA-binding functional surface (ADR) variants, encompassing a fully randomized library of positions Y17, Q18, and R22 (YQR). This library was tested against 64 putative operator variants, with the sequence 5′-A ATT $\vartheta\vartheta\vartheta$ AGC GCT ΨΨΨ AAT T-3′, where ϑ is any nucleotide, and Ψ is the complement necessary to achieve full (palindromic) symmetry. Each putative DNA operator typically had multiple ADR complements. We posited that a DNA binding domain substitution could be identified to replace an existing ADR to facilitate improved performance of a given TF system. Accordingly, we sought DNA binding domain variants that (i) only had one reported interaction with the DNA operator of interest, and (ii) the performance metrics were similar to the basis ADR being replaced. Using this criteria NAR had one putative replacement (LAR), TAN and GKR had two putative replacements each (HAN, IAN, and FKR, IKR, respectively), whereas HTK had no apparent replacements. In addition, we identified two additional ADR (ICK and IAY) that paired with a new DNA operator (O^{cta}), potentially allowing us to expand the original matrix.

Initially, we focused on pairing a transcription factor to the O^{gta} operator, as the $P^A_{NAR}|O^{gta}$ unit operation (i) cannot interact with the cognate operator, and (ii) the dynamic range is significantly less than 5 (observed as 1.3 as tested). Here, we exchanged the alternate DNA binding domain NAR with LAR. The resulting P^A_{LAR} transcription factor interacted with the cognate operator O^{gta} and functioned as an antirepressor with a dynamic range of 5.04. Next, we sought to improve the performance of the antirepressor directed toward O^{gac}, as the initial unit operation ($P^A_{GKR}|O^{gac}$) had the next lowest cognate fold induction at 1.61. We explored two variants to GKR—*i.e.*, IKR, and FKR. In both cases, the replacement unit operations $P^A_{IKR}|O^{gac}$ and $P^A_{FKR}|O^{gac}$ interacted with the cognate operator

https://dx.doi.org/10.1021/acssynbio.0c00582
ACS Synth. Biol. 2021, 10, 552−565

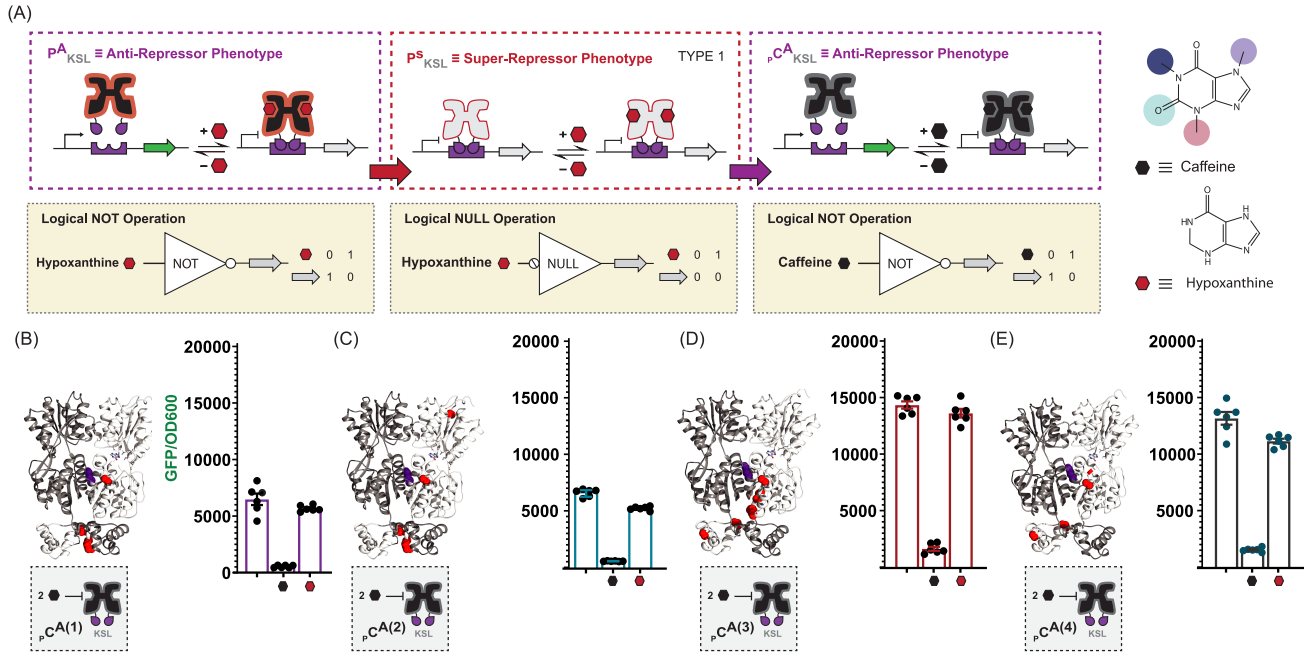

Figure 2. Workflow for engineering caffeine responsive transcription factors. (A) Caffeine specificity was evolved in the P^A scaffold *via* a type-I super-repressor intermediate (logical NULL operation). For a type-I super-repressor, the binding pocket is left intact and the mutations impose a block in the allosteric communication of the protein. Performance for (B) ${}_PC^{A(1)}{}_{KSL}$, (C) ${}_PC^{A(2)}{}_{KSL}$, (D) ${}_PC^{A(3)}{}_{KSL}$, (E) ${}_PC^{A(4)}{}_{KSL}$ along with the mutations introduced shown on the PurR crystal structure (PDB ID 2PUD). *Y*-axis is given as GFP/OD_{600}, which is calculated by taking GFP fluorescence (485 ex., 510 em.) normalized to OD_{600} for each well. Each value corresponds to the mean of $n = 6$ biological replicates and error bars indicate the standard error of the mean (SEM). Note: The difference in the expression in the control normalized GFP outputs (*i.e.*, minus ligand) is due to variation in low-affinity interactions of the transcription factors in the absence of ligand.

(O^{gac}) with a dynamic range of 7.4 and 11.1, respectively. In turn, we evaluated both replacements for TAN (*i.e.*, HAN and IAN). The HAN replacement directed to the O^{ttg} operator had a cognate dynamic range of 5.03. However, this system had multiple off diagonal (noncognate) interactions, and thus was excluded as a replacement. In contrast, the IAN replacement (on O^{tta}) had a dynamic range of 1.03, and was also excluded based on poor performance. Finally, the natural LacI DNA binding domain (YQR) interacts with the native O^1 operator along with the symmetric O^{sym} operator. Previous studies have shown that $I^+{}_{YQR}$ paired with O^{sym} increased the dynamic range of this unit operation.[18,20,31] The O^{sym} DNA operator is a symmetric variant of O^1. Specifically, in the O^{sym} DNA element the right side has been mutated to match the left side of the operator resulting in perfect palindromic symmetry. The architecture is congruent with the symmetric configuration used to design the six foundational ADR operators. Accordingly, we surmised that a similar improvement would be observed for the $P^A{}_{YQR}$ antirepressor paired with O^{sym}, which was evidenced by an observed dynamic range of 6.92. In summary, the aforementioned changes resulted in three additional systems (5 in total) with performance metrics *on par* (or better than) the reference system ($I^+{}_{YQR}|O^1$), see Figure 1F. In addition, we expanded the set of orthogonal TF|operators *via* the pairing of $P^A{}_{ICK}|O^{cta}$, though the system was not perfectly orthogonal. Given that protein−DNA interaction design rules could not be established based on the broader study from Milk *et al.*, a quantitative explanation for the observed increases in the dynamic ranges were difficult to reconcile completely. We posited that improved pairing of allosteric networks with alternate DNA binding domains could account for much of the improved performance, consistent with the arguments we posed previously.[31,67] To reconcile an improvement in dynamic range would require a complete assessment of the permissive allosteric network, which is beyond the scope of this study.

Part II: Blocking Allosteric Communication in the PurR Parent Scaffold. Given the structural similarities between hypoxanthine (*i.e.*, the cognate ligand to PurR) and other methylxanthines—*e.g.*, caffeine (1,3,7-trimethylxanthine)—we hypothesized that the purine repressor could be engineered to recognize and allosterically respond to caffeine and similar derivatives. We posited that functional ligand binding in the LacI/GalR topology is inextricably linked to allosteric communication.[67] Accordingly, we surmised that the corresponding engineering workflow to confer alternate ligand (caffeine) binding and allosteric response in the PurR topology will likely require correlated changes in the allosteric network. From the standpoint of forward design, ligand binding is often regarded as a local phenomenon (design problem) in which the residues that come into direct contact (or are within the proximal environment to) the ligand only need be considered. In this study, we are interested in engineering allosteric TFs. Accordingly, protein design that strictly focuses on ligand binding will likely yield moderate (if any) results, as evidenced in previous studies[63] and observed in our unpublished reports. Given that the *a priori* design of an allosteric network is currently intractable, we conceded that a strategy that included laboratory evolution would offer the most promising path toward a pragmatic solution(s) to our design goal.

Previously, we have demonstrated that alternate allosteric communication could be conferred in several LacI/GalR scaffolds, resulting in the inversion of function—*i.e.*, transitioning from the repressor to the antirepressor phenotype.[29,31,68] In

https://dx.doi.org/10.1021/acssynbio.0c00582
ACS Synth. Biol. 2021, 10, 552−565

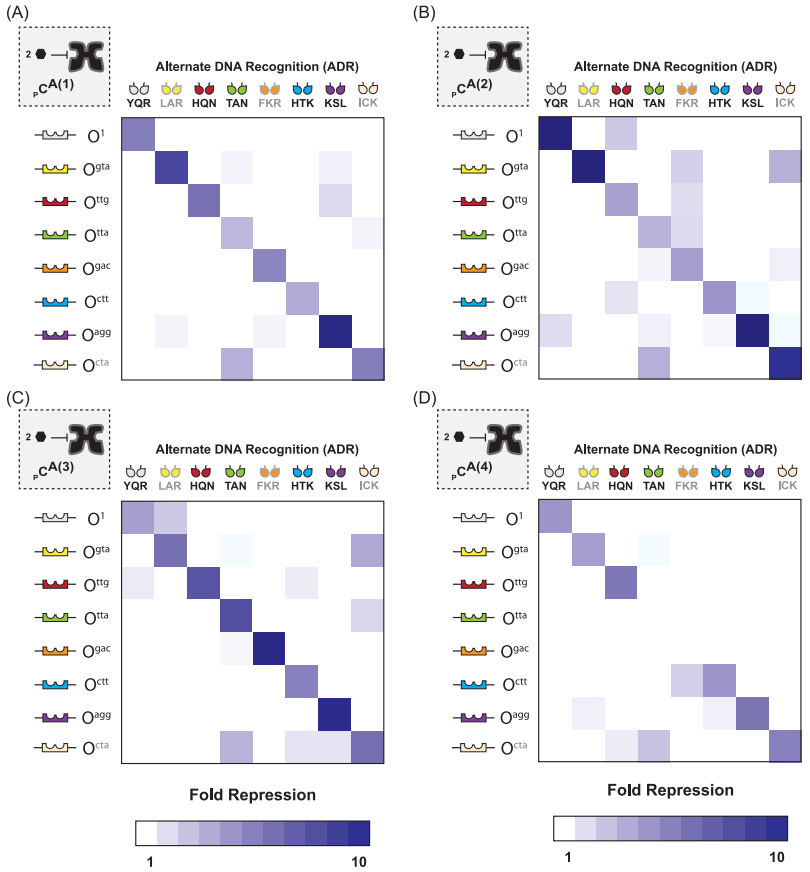

Figure 3. Engineered antirepressors with alternate DNA recognition (ADR). Heatmaps illustrating the dynamic range of each ADR-operator pair for (A) ${}_{P}C^{A(1)}$, (B) ${}_{P}C^{A(2)}$, (C) ${}_{P}C^{A(3)}$, (D) ${}_{P}C^{A(4)}$.

this engineering workflow, first we introduced a block in allosteric communication resulting in a super-repressor phenotype. In turn, we introduced compensatory mutations *via* error-prone PCR (EP-PCR) to confer antirepression in the given scaffold. We surmised that we could leverage a similar engineering workflow to confer both alternate ligand (caffeine) binding and complementary alternate allosteric response in the PurR scaffold. Moreover, given that our resulting library of mutants will be enriched with alternate allosteric networks, we posited that functional variants would possess greater specificity to the target ligand (caffeine), as the resulting alternate allosteric networks are not necessarily optimal for the original ligand (provided we focus our discovery on the ligand of choice).

For the initial step of this engineering strategy, we first normalized DNA binding function by introducing a common DNA binding domain, which is generally the native lactose repressor domain, YQR. However, we have consistently observed that the KSL DNA binding domain paired with its cognate operator (O^{agg}) yields transcription factor variants with desirable performance characteristics across a variety of protein scaffolds.[18,31] Namely, KSL variants (repressors or antirepressors) typically interact exclusively with the cognate DNA operator and display dynamic ranges greater than 5. Accordingly, we decided to use ${P^{A}}_{KSL}$ as the parent scaffold, rather than the previously reported ${P^{A}}_{YQR}$ chimera. Initially, we used a primary sequence alignment to identify putative super-repressor positions in the ${P^{A}}_{KSL}$ scaffold (Supplementary Figure S1). Point-mutation to positions 84, 88, 95, and 96 in LacI have been shown to confer super-repression, without neutralizing the ligand binding site.[29,31,68] In a recent report,[31] we illustrated that many of these positions are conserved in other LacI/GalR homologues. Accordingly, we performed saturation mutagenesis at each amino acid position corresponding to 84, 88, 95, and 96 in the ${P^{A}}_{KSL}$ scaffold. Unfortunately, we did not observe the super-repressor phenotype within the finite sequence space.

Mechanistically, engineering a super-repressor is (in principle) more challenging when starting with a native antirepressor, as the mutation needs to not only impose a block in allosteric communication, but also shift the conformational equilibrium of the protein into the high DNA affinity state, which in the case of PurR, occurs in the presence of ligand. Notably, the point-mutation K84A potentially achieved both criteria in the LacI topology—as evidenced by several biochemical and biophysical studies[69,70]—in contrast to the aforementioned mutations, which only block the propagation of the allosteric signal. Accordingly, we opted to identify the corresponding position in PurR *via* structural alignment of LacI (1EFA) and PurR (2PUD) both in the DNA bound conformation, positing that amino acid identity and three-dimensional position are required in the identification of this critical position. Upon inspection of the alignment we found that PurR has a lysine at position 85 (K85), which appears to play a similar functional role at the monomer−monomer interface (Supplementary Figure S2). Saturation mutagenesis at amino acid position 85 yielded at least one super-repressor variant K85S (or approximations thereof—*e.g.*, K85A), which

https://dx.doi.org/10.1021/acssynbio.0c00582
ACS Synth. Biol. 2021, 10, 552−565

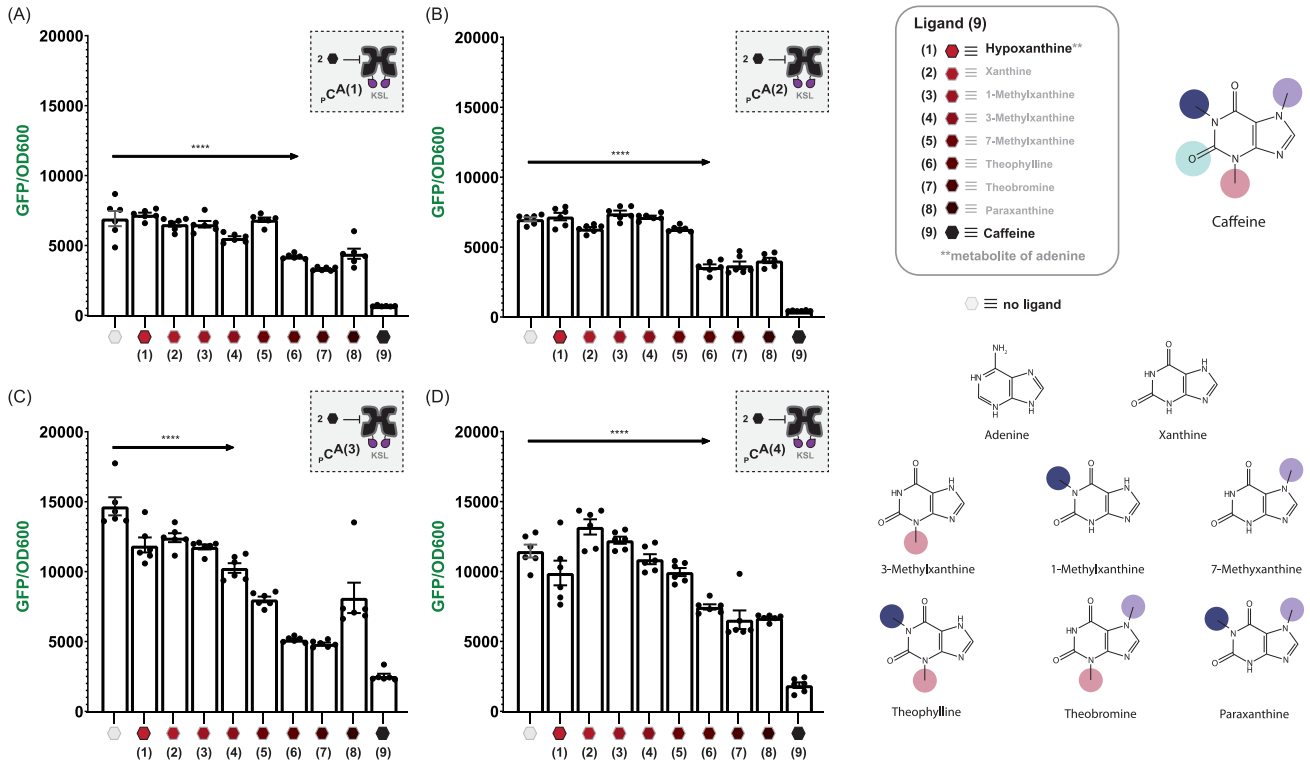

Figure 4. Probing ligand specificity of engineered antirepressors. Measured response of (A) ${}_{P}C^{A(1)}{}_{KSL}$, (B) ${}_{P}C^{A(2)}{}_{KSL}$, (C) ${}_{P}C^{A(3)}{}_{KSL}$, (D) ${}_{P}C^{A(4)}{}_{KSL}$ toward a variety of compounds whose structures resemble either caffeine or the native ligand, adenine. The structure of each of the 9 ligands tested is depicted and each ligand is represented by a different color. The concentration of each ligand is 1 mM except for adenine, which was used at 0.6 mM (solubility). *Y*-axis is given as GFP/OD_{600}, which is calculated by taking GFP fluorescence (485 ex., 510 em.) normalized to OD_{600} for each well. Each value corresponds to the mean of $n = 6$ biological replicates and error bars indicate the SEM. All values to the right of the (****) arrowhead indicate statistical significance at the $\alpha = 0.0001$ level using a one-way ANOVA followed by a *post hoc* Dunnett's Test using the "No Inducer" condition as a control.

displays repressed gene output in the absence of ligand as well as in the presence of either hypoxanthine or caffeine (Figure 2A).

Part III: Conferring Alternate Ligand (Caffeine) and DNA Binding Responsiveness. Using the K85S ${P^{S}}_{KSL}$ super-repressor as the starting point we conducted a single round of EP-PCR with a mutational rate between 1 and 4, followed by a screen monitoring regulated GFP output. Here the objective was to engineer and identify variants that were responsive (as antirepressors) to the ligand caffeine, with mitigated responsiveness to the native ligand hypoxanthine (*i.e.*, a metabolite of adenine). Our initial round of EP-PCR (starting with K85S ${P^{S}}_{KSL}$) yielded a single variant (${}_{P}C^{A}{}_{KSL}{}^{(K85S/A99T)}$) which was responsive to caffeine. However, the ${}_{P}C^{A}{}_{KSL}{}^{(K85S/A99T)}$ antirepressor variant—while responsive to the ligand caffeine—only had a dynamic range of 2.1 (*i.e.*, significantly below the reference value of 5). In a previous study, Meinhardt *et al.* demonstrated that modifications to the hinge region of the DNA binding domain could improve the performance of TFs with the PurR topology.[71] Likewise, we posited that additional modifications to the hinge region (*i.e.*, residues V52, S55, Q60, and K62) of the ${}_{P}C^{A}{}_{KSL}{}^{(K85S/A99T)}$ antirepressor variant could improve the dynamic range. Accordingly, we fully randomized the four positions 52, 55, 60, and 62 with NNK degenerate codons in tandem with a second round of EP-PCR. Using a combination of fluorescence assisted cell sorting (FACS) and microwell plate assay we identified four variants (${}_{P}C^{A(1-4)}{}_{KSL}$) with the desired performance metrics—*i.e.*, (i) anti-induction in the presence of caffeine, with greater than 5 fold anti-induction, and (ii) abrogated responsiveness to hypoxanthine (Figure 2B–E). All variants retained a mutation at allosteric position K85 (S or A), in addition to the A99T conferred mutation. Moreover, each of the four variants contained some variation in the hinge-helix region of the DNA binding domain (Supplementary Figure S3). Consistent with our initial hypothesis alternate ligand binding was achieved by way of alternate allosteric routes, rather than variation in the constellation of residues that are responsible for ligand binding (*i.e.*, excluding residues I249, E222, D220, F221, Y73, F74, S124, also see Supplementary Figure S2). Moreover, each of the resulting caffeine responsive antirepressors (${}_{P}C^{A(1-4)}{}_{KSL}$) had mitigated responsiveness to the original ligand hypoxanthine, with no evidence of antagonistic rejection of the cognate (caffeine) input (Supplementary Figure S3).

In principle, alternate DNA binding can be conferred in each of the four engineered caffeine responsive antirepressors using the modular design strategy outlined in Figure 1. Moreover, we have observed in our previous studies that DNA binding adaptation to disparate DNA operators of a given transcription factor (repressor or antirepressor) can also influence the dynamic range. Using the same ADR set—though adapted over the modifications to the hinge-helix region for each base antirepressor—we generated a total of 32 putative antirepressor variants, or 28 additional variants excluding KSL. Approximately 94% of the variants functioned as cognate

https://dx.doi.org/10.1021/acssynbio.0c00582
ACS Synth. Biol. 2021, 10, 552–565

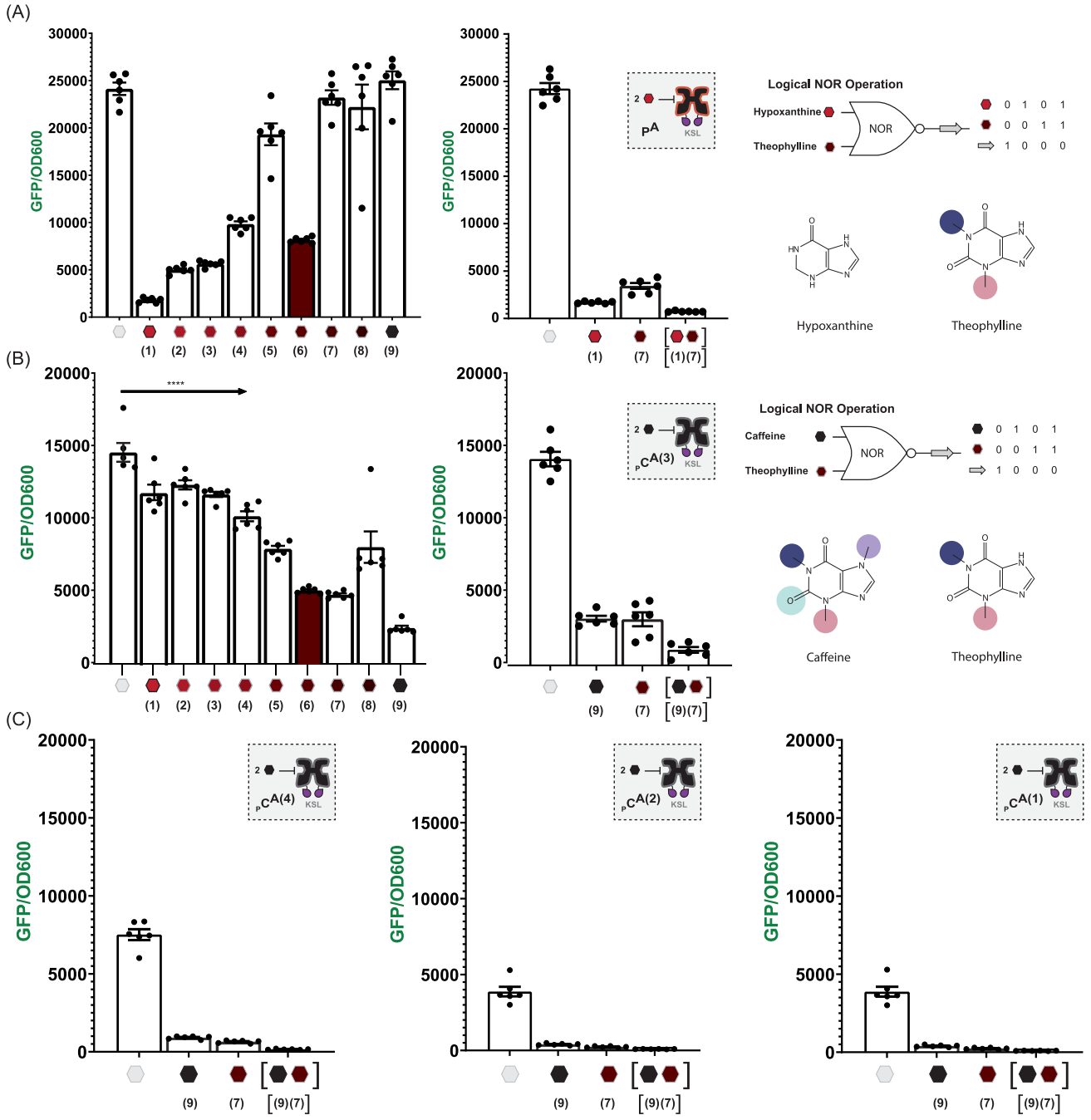

Figure 5. Constructing NOR logical operations. (A) Measured response of P^{A}_{KSL} toward a variety of compounds whose structures resemble either caffeine or the native ligand, adenine. P^{A}_{KSL} demonstrates a strong response toward theophylline (shown in purple), along with its native ligand, adenine, which can be used to build a logical NOR operation. (B) Similarly, ${}_{P}C^{A(3)}{}_{KSL}$ responds to theophylline as well as caffeine, allowing for a slightly different NOR operation. (C) NOR gates built using each of the remaining ${}_{P}C^{A}{}_{KSL}$ variants responding to caffeine and theophylline. *Y*-axis is given as GFP/OD_{600}, which was calculated by taking GFP fluorescence (485 ex., 510 em.) normalized to OD_{600} for each well. Each value corresponds to the mean of $n = 6$ biological replicates and error bars indicate the SEM. All values to the right of the (****) arrowhead indicate statistical significance at the $\alpha = 0.0001$ level using a one-way ANOVA followed by a *post hoc* Dunnett's Test using the "No Inducer" condition as a control. Note: In all of the reported NOR gates the concentration of theophylline has been increased to 2 mM to improve the dynamic response.

${}_{P}C^{A}{}_{ADR}$ antirepressors (see Figure 3, also see Supplementary Figure S4–S5). Only 2 ADR variants failed to produce functional transcription factors (${}_{P}C^{A(4)}{}_{TAN}$ and ${}_{P}C^{A(4)}{}_{FKR}$). Interestingly, in each of the four performance matrixes the variants adapted with KSL had the largest dynamic range. However, in all cases variants adapted with ADR resulted in an increase in the number of noncognate interactions relative to the PurR parent matrix shown in Figure 1F. We also measured the dose response for each of the transcription factors, Supplementary Figure S4. No discernible trends emerged with regard to caffeine sensitivity that was consistent between groups of antirepressors functioning on cognate operators. This observation is consistent with our hypothesis that

https://dx.doi.org/10.1021/acssynbio.0c00582
ACS Synth. Biol. 2021, 10, 552–565

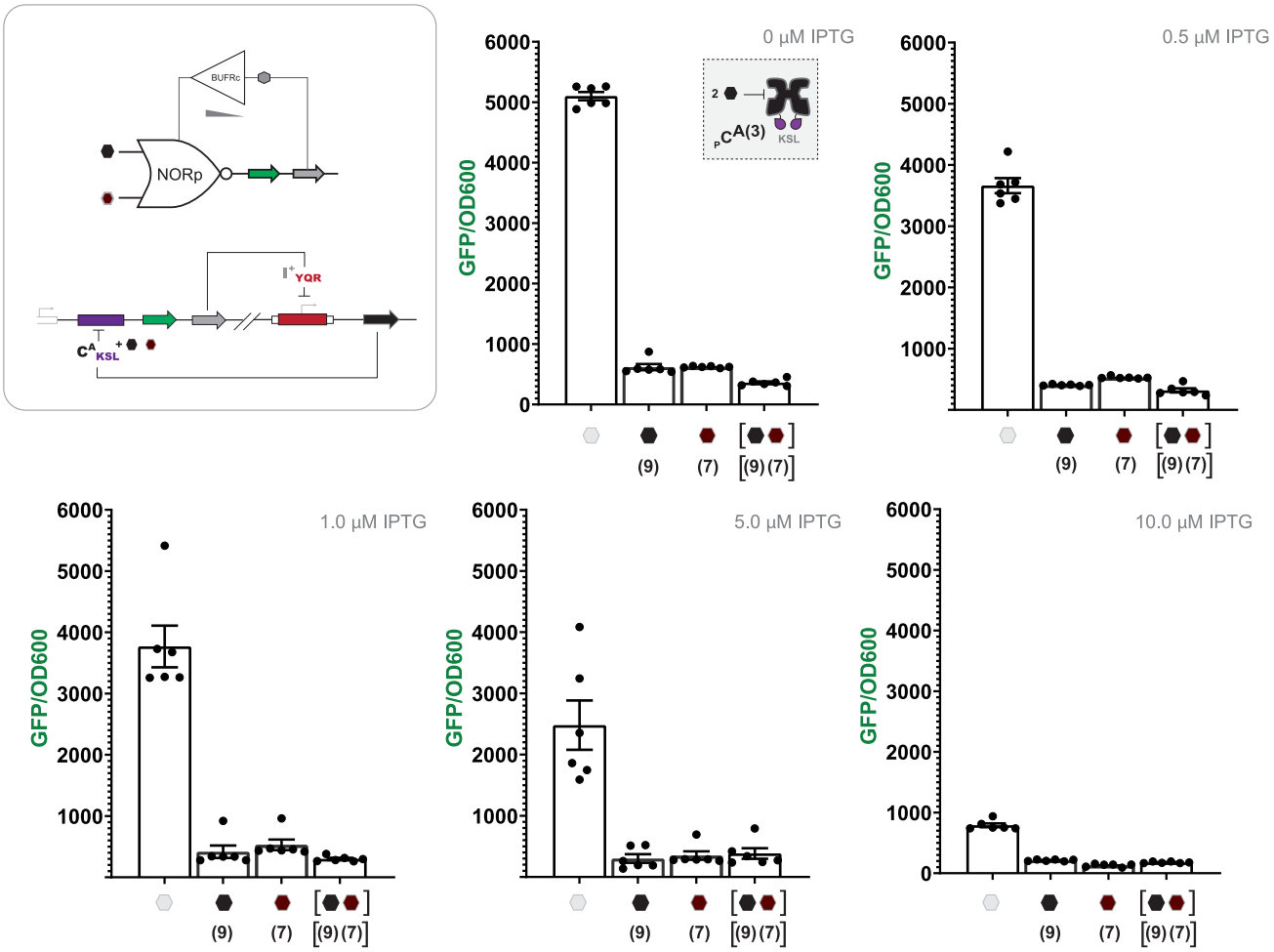

Figure 6. Dynamically tunable NOR operations. Feedback control can be incorporated into the NOR operation by coupling GFP output to the production of a second transcription factor, I^{+}_{HQN}. This TF will then serve as a buffer (BUFR) to modulate expression levels of the antirepressor, ${}_{P}C^{A}_{KSL}$. The concentration of the ligand IPTG alters the affinity of I^{+}_{HQN} for its operator, thereby affecting overall expression of ${}_{P}C^{A}_{KSL}$, allowing for dynamic tuning of overall circuit performance. *Y*-axis is given as GFP/OD_{600}, which was calculated by taking GFP fluorescence (485 ex., 510 em.) normalized to OD_{600} for each well. Each value corresponds to the mean of $n = 6$ biological replicates and error bars indicate the standard error of the mean (SEM). Note: The complexity of information processing *via* such systems will likely have a putative upper-limit of approximately 4 transcription factors in a given chassis cell, due to toxicity issues.[18]

allosteric network and ADR pairing have a (yet undetermined) impact on functional outcomes. Collectively, this system of transcription factors contains at least one antirepressor variant with alternate DNA binding that interacts exclusively with one (cognate) DNA operator. Thus, we have achieved the development of an orthogonal set of 7 (plus 1 ICK) ${}_{P}C^{A}_{ADR}$ antirepressors (responsive to caffeine) that can be used in collaboration with our broader set of engineered repressors[18,20] and antirepressors,[31] in addition to the set of 7 (plus 1 ICK) P^{A}_{ADR} antirepressors shown in Figure 1F.

Part IV: Evaluating Antirepressor Specificity and Dynamically Tunable Logical Operations. While our primary engineering goal was successful—*i.e.*, conferring antirepressor responsiveness to the ligand caffeine, while mitigating binding and action to hypoxanthine—we wanted to determine to what extent our engineered transcription factors could interact an respond to other methylxanthines (or caffeine metabolites) with similar chemical structures; see Figure 4. Here we selected ${}_{P}C^{A}_{KSL}$ antirepressors as these transcription factors had the best performance metrics (*i.e.*, dynamic ranges) observed in this study. Here, we assessed responsiveness of each of the ${}_{P}C^{A}_{KSL}$ antirepressors to seven methylxanthine derivatives (xanthine, 1-methylxanthine, 3-methylxanthine, 7-methyxanthine, theophylline, theobromine, and paraxanthine) at a fixed ligand concentration of 1 mM. Rather than using our standard GFP reporter system, we employed a variation in which superfolder GFP was paired with the weak LDA degradation tag, as we found that this increase the dynamic range by decreasing basal expression (*i.e.*, reducing leakiness), see Supplementary Figure S6. This change provides greater sensitivity when probing ligand response and could serve to highlight weaker interactions.

In Figure 4, the ligand concentrations were restricted to 1 mM for the seven methylxanthine derivatives (due to solubility limits for several of the putative ligands), and caffeine was also restricted to 1 mM to facilitate a more accurate relative comparison. In general, none of the methylxanthine derivatives demonstrated better relative performance than caffeine for any of the ${}_{P}C^{A}_{KSL}$ antirepressors. Methylxanthine derivatives closer in chemical structure to caffeine had a moderate anti-inductive

https://dx.doi.org/10.1021/acssynbio.0c00582
ACS Synth. Biol. 2021, 10, 552−565

response on each of the $_{P}C^{A}_{KSL}$ transcription factors (*i.e.*, theophylline, theobromine, and paraxanthine). This is in contrast to, the response of the parent transcription factor P^{A}_{KSL}, which shows a much stronger response toward the native ligand hypoxanthine as well as the molecules xanthine, 1-methylxanthine, and 3-methylxanthine—*i.e.*, derivatives that are closer in chemical structure to hypoxanthine (Figure 5A). Note, guanine (*i.e.*, one of two native ligands to PurR) was excluded from this study due to solubility issues.

Interestingly, the P^{A}_{KSL} and the four $_{P}C^{A}_{KSL}$ antirepressors all responded to theophylline, which can be regarded as a chemical intermediate between hypoxanthine and caffeine. Moreover, increasing the concentration of theophylline to 2 mM improved the dynamic response of all antirepressors—*i.e.*, bringing the dynamic range for P^{A}_{KSL} and the $_{P}C^{A}_{KSL}$ antirepressors approximately *on par* with the cognate ligand (hypoxanthine or caffeine) response for each antirepressor; see Figure 5A. Balancing the dynamic range in response to these ligands enabled us to consider the construction of an important Boolean logical operation, NOR. The NOR gates presented in Figure 5 represent an important iteration on our most recent next-generation NOR operations that eliminate the need for inversion.[31] In this example, in addition to the elimination of the inversion step we have reduced this unit operation to a single two-signal responsive transcription factor—*i.e.*, opposed to two separate antirepressors that respond to two disparate signal inputs directed toward a single DNA operator. Namely, the P^{A}_{KSL} antirepressor was responsive to hypoxanthine and theophylline, and in the presence of one or both signals the output (GFP) was not produced (Figure 5A), whereas, the $_{P}C^{A}_{KSL}$ antirepressors were responsive to caffeine and theophylline with a similar NOR functionality, in which the output was rejected when one or both ligands (*i.e.*, caffeine and/or theophylline) were present; see Figure 5B,C.

Although synthetic genetic circuits allow us to modify the behavior of living cells, the behavior of many regulatory components making up these circuits is sensitive to many factors such as differences in host physiology[72−74] and interactions between genetic parts and the host cell.[75−78] As a result, genetic circuits must often be reassembled multiple times until a working combination of parts is found, which can be time-consuming, labor-intensive, and costly. To tackle this problem, we have developed transcriptional-mediated feedback control systems (Figure 6 and Supplementary Figure S7) that allow for the dynamic tuning of steady-state response functions to correct for unwanted changes in circuit behavior. Feedback was implemented *via* the coupled expression of the output (GFP) to the expression of a second TF (I^{+}_{HQN}), which modulated the expression of the $_{P}C^{A(3)}_{KSL}$ antirepressor regulating the output. In the absence of ligand, relatively high levels of I^{+}_{HQN} are produced, which led to repression of the $_{P}C^{A(3)}_{KSL}$ and consequent increase in GFP expression (as well as I^{+}_{HQN}). Conversely, in the presence of the corresponding ligand, the $_{P}C^{A(3)}_{KSL}$ diminished the production of I^{+}_{HQN} thereby leading to an increase of $_{P}C^{A(3)}_{KSL}$ and stronger antirepression of the final GFP output. Thus, this feedback loop functioned to amplify the response of the engineered $_{P}C^{A(3)}_{KSL}$ transcription factor. By using the two ligands caffeine and theophylline, we can illustrate the utility of these feedback loops by developing a NOR gate with tunable transitions between the "ON" and "OFF" states, which will make them more broadly compatible with other components.[79,80] Similar tunable feedback systems can be constructed that are sensitive to caffeine and chocolate (theobromine); see Supplementary Figure S7.

DISCUSSION

Fueled by advances in synthetic biology, microbiology, ecotoxicology, and microsystems engineering, the field of whole-cell bacterial bioreporters has quickly developed the ability to detect and quantify a wide array of components ranging from toxic chemicals to valuable metabolites. Accordingly, bacterial cell-based sensors have been studied for various applications, such as environmental monitoring,[6−8] disease diagnosis,[9−11] and bioproduction.[81−83] Unlike traditional physical or chemical sensors, cellular sensors have the added benefits of being highly selective, easy to manufacture, cost effective, and renewable,[84,85] contributing to a more sustainable future. In general, a whole cell-based biosensor consists of a module that senses the input signal and a reporter module that converts the biosensor input into an output signal, all within a chassis cell that implements the designed devices.[84,85] Traditionally, the sensing components in these circuits came exclusively from existing signaling pathways, but despite the seemingly endless diversity of these natural components, some cases have warranted synthetic approaches to detect a particular chemical target.[64,85−87]

Caffeine (1,3,7-trimethylxanthine) is one of the most popular and commercially important plant-derived purine alkaloids.[88] This ubiquitous small molecule is a key component of widely consumed beverages, such as coffee, tea, soft drinks, energy drinks[89] and is an additive to over 150 food and 570 drink products currently on the market.[90] Caffeine can be regarded as an addictive substance,[91] and recent studies suggest that long-term and excessive consumption of caffeine can lead to various adverse health effects.[92] The FDA considers a concentration of caffeine above 200 ppm or 0.02% in foods and beverages to be unsafe [*21 Code of Federal Regulations, section 182.1180(b)*]. Due to the omnipresence of this methylxanthine variant in modern society, caffeine concentration in wastewater has been identified as an accurate marker of anthropogenic burden and pollution.[93,94] Taken together, these points highlight the need for a simple, quick, and cost-effective method to detect caffeine, which we posited can come in the form of a whole-cell biosensor based on a bespoke antirepressive transcription factor.

Recently, several caffeine biosensors have been developed;[54,55] however, none are based on allosteric transcription factors. The benefit of engineering a system of allosteric transcription factors that respond to caffeine would not only serve as the foundation for a biosensor, but could also seamlessly integrate into our growing collection of engineered TFs and our emerging transcriptional programming edifice.[18,31] Accordingly, our design goals for the resulting system of novel antirepressors was evident—*i.e.*, responsiveness to caffeine, with mitigated sensitivity to the native ligand and native DNA operator. To this end, we have engineered a collection of 28 novel antirepressors (4 systems, composed of 7 alternate DNA binding functions) with varying degrees of responsiveness toward the non-natural ligand caffeine. Moreover, specificity toward the native ligand was mitigated, which stands in stark contrast to many other attempts to alter ligand specificity in similar scaffolds.[62−64] As this system of antirepressors stand, these engineered TFs could serve as the basis of a whole-cell caffeine biosensor. In addition, consequent rounds of directed evolution can be employed to engineer

https://dx.doi.org/10.1021/acssynbio.0c00582
ACS Synth. Biol. 2021, 10, 552−565

properties commensurate with the user's needs (*e.g.*, better specificity and sensitivity).

Although our original design goal was to evolve our proteins to recognize caffeine, there are several other methylxanthines that would be important to detect. Specifically, paraxanthine (1,7-dimethylxanthine) exerts physiological effects similar to caffeine not only as a stimulant, but also as a modulator of immune function and inflammation.[95] In addition, theophylline (3,7-dimethylxnanthine) and theobromine (1,3-dimethylxanthine) are pharmaceutically active molecules that serve as bronchodilators and are commonly used asthma medications.[96] Many of the traditional methods used to detect these molecules are invasive, expensive, and laborious, often requiring highly specialized operators and sophisticated instrumentations. As can be seen in Figure 4, the four transcription factors engineered in this work respond not only to caffeine, but are moderately responsive to dimethylxanthines paraxanthine, theophylline, and theobromine. Likewise, the parent P^{A}_{KSL} scaffold shows moderate response toward the molecules xanthine, 1-methylxanthine, 3-methylxanthine, and 7-methylxanthine. Accordingly, our current and future efforts are focused on expanding our collection of TFs to be specifically responsive to varying methylxanthines beyond caffeine.

MATERIALS AND METHODS

Vector Construction and Reporter Systems. All transcription factor variants were inserted into the pLacI plasmid (Novagen), which contains a low copy number p15A origin, a chloramphenicol resistance marker, and the gene for the repressor regulated with a constitutive LacI promoter. The coding sequence for the LacI:PurR chimera LLhP 48/57−61 was obtained from previous work by Tungtur *et al.*[61] and synthesized by Eurofins Genomics. This open reading frame (ORF) was amplified *via* PCR and inserted into the pLacI vector using circular polymerase extension cloning (CPEC). Mutations to the DNA-binding domain were then introduced *via* routine site-directed mutagenesis using Phusion DNA polymerase with GC buffer (New England Biolabs). For each repressor variant, the entire gene reading frame along with the promoter driving expression was sequenced in the forward and reverse direction (Eurofins Genomics) to verify all mutations and correct assembly. To measure control over gene expression, a reporter plasmid system was constructed as outlined previously.[20] This plasmid contains the low copy number pSC101* origin of replication, a kanamycin resistance marker, along with superfolder green fluorescent protein (sfGFP) driven by the constitutive *trc* promoter. The operator region lies 5bp downstream of the promoter element and each operator variant was constructed using site-directed mutagenesis. When used, the ssra-LDA degradation tag was incorporated using inverse PCR followed by treatment with KLD Enzyme Mix (NEB). Detailed sequence data—*i.e.*, promoter sequences, transcription factors, and vector maps—are given in Supplementary Figure S6.

Microplate Assay for Gene Expression. All experiments were performed in the cell strain 3.32[97] (Genotype lacZ13-(Oc), lacI22, LAM−, el4−, relA1, spoT1, and thiE1, Yale CGSC #5237), an *E. coli* K12 strain with LacI and the lac operon deleted. The plasmids were cotransformed and plated on LB agar with the appropriate antibiotics (chloramphenicol for pLacI, ampicillin for pSO, and kanamycin for the reporter plasmid). The necessary plasmids were cotransformed and plated onto LB agar with the appropriate antibiotics (chloramphenicol for pLacI and kanamycin for the reporter plasmid). For the microplate assays, individual colonies were inoculated in 1 mL of LB and grown overnight at 37 °C with shaking at 300 rpm After this initial growth period, cultures were diluted into 200 μL wells in M9 minimal Media supplemented with 0.2% casamino acids, 1 mM thiamine HCl, 100 μM $CaCl_2$, and 2 mM $MgSO_4$ along with the appropriate antibiotics and the corresponding effector ligands. Ligands used are as follows: adenine from Acros Organics CAS 73−24−5, caffeine from Chem-Impex International CAS 58−08−2, xanthine from Sigma-Aldrich CAS 69−89−6, 1-methylxanthine from Sigma-Aldrich CAS 6136−37−4, 3-methylxanthine from Carbosynth CAS 1076−22−8, 7-methylxanthine from Carbosynth CAS 552−62−5, paraxanthine from Carbosynth CAS 611−59−6, theobromine from Alfa Aesar CAS 83−67−0, and theophylline from Sigma-Aldrich CAS 58−55−9. Except where otherwise indicated, ligands were used at a final concentration of 1 mM. Biological replicates were aliquoted into six samples in a clear, sterile, conical-bottom 96-well plate (Fisher Scientific) and grown in a 37 °C shaker at 300 rpm covered with a Breathe-Easier sealing membrane (Midwest Scientific) to prevent evaporation. Cells were transferred to a black 96-well plate (COSTAR) during exponential growth phase (approximately 16 h) for assaying. GFP fluorescence (ex. 485 nm, em. 510 nm, gain 50) and optical density (OD_{600}) were measured using a Synergy HT plate reader (BioTek). Corrections for path length were made using OD_{900} and OD_{975} and the fluorescence values were normalized to the optical density and averaged across all biological replicates. For each operator variant, the maximum GFP expression was determined using the LacStop control plasmid.[18]

Structural Analyses and Depiction. All structure depictions were created using UCSF Chimera.[98] Structural alignments were completed using the Match → Align function.

Protein Library Creation. All site-saturation mutagenesis was performed using an inverse PCR with NNK degenerate codons; NNK was chosen as this allows for full codon coverage while limiting the possibility of premature STOP codons. Following treatment with KLD Enzyme Mix (NEB), product was transformed into NEB 5-alpha competent cells. The library was streaked and cultured for plasmid isolation and the DNA was sequenced to verify saturation at the desired site. The directed evolution library was constructed using a protocol adapted from Richards *et al.*[29] The entire coding sequence of the P^{S}_{KSL} variant K85S—excluding the DNA binding domain (DBD)—was subjected to error-prone PCR (residues 25−343). The DBD was intentionally excluded, as mutations in this region are mainly responsible for DNA recognition, rather than ligand specificity. A library with 5 bp to 7 bp (1−4 residue) mutations, on average, over the 1100 bp region, was constructed in a reaction with 1.25 U Taq DNA Polymerase (NEB), 1× Taq Mg-free buffer (NEB), 1.8 mM MgCl2 (NEB), 200 μM MnCl2 (Millipore Sigma), 0.4 μM dCTP (NEB), 0.4 μM dTTP (NEB), 0.08 μM dGTP (NEB), 0.08 μM dATP (NEB), 500 μM, each, forward and reverse primers, and 10 ng (4.2 fmol) of P^{A}_{KSL} DNA, as a template. The reaction was subjected to 95 °C for 3 min and 20 cycles of 95 °C for 30 s, followed by 68 °C for 5 min, and a final extension at 68 °C for 10 min. In a separate PCR, the LacI vector (containing the pLacI promoter and residues 1−25) was linearized and both products were visualized on an agarose gel.

https://dx.doi.org/10.1021/acssynbio.0c00582
ACS Synth. Biol. 2021, 10, 552−565

The EP-PCR insert was gel extracted (Qiagen) and then reamplified using Phusion Polymerase (NEB), while the vector was treated with DPNI (NEB) to eliminate any residual template. The two fragments were combined *via* CPEC and transformed into NEB 5-alpha competent *E. coli* (huA2 Δ(argF-lacZ)U169 phoA gln *V*44 φ80Δ(lacZ)M15 gyrA96 recA1 relA1 endA1 thi-1 hsdR17; New England Biolabs). The library size was estimated to be on the order of 10^6 colony forming units (cfu).

Fluorescence Assisted Cell Sorting (FACS). Colonies were inoculated in LB with relevant antibiotics (chloramphenicol for pLacI, kanamycin for the GFP reporter) and grown overnight at 37 °C, shaking at 300 rpm. Cultures were then diluted 1:100 in supplemented M9 minimal Media containing relevant antibiotics and ligands in sterile culture tubes (Nunc) and grown at 37 °C, shaking at 300 rpm until cells reached exponential phase. Each culture was then aliquoted such that the optical density (OD_{600}) would be approximately equal to 0.2 (WPA Biowave CO8000 Cell Density Meter) in the final solution volume (typically 1 mL). Cells were then pelleted at 14 000 rpm for 2 min (Beckman Coulter Microfuge 18). The supernatant was then discarded, and cells were resuspended in PBS supplemented with 25 mM HEPES (Fisher Scientific), 1 mM EDTA (Millipore Sigma), and 0.01% (v/v) Tween20 (VWR Life Sciences), and again pelleted at 14 000 rpm for 3 min. This wash step was repeated once before cells were finally resuspended in PBS supplemented with 25 mM HEPES and 1 mM EDTA.

Cytometry experiments were performed as outlined in Groseclose *et al.*[31] using a BD FACSAria Fusion flow cytometer (BD Biosciences) equipped with a 100 mW 488 nm laser for excitation, a 510/30 nm bandpass emission filter, and an 85 μm nozzle. Cells were interrogated measuring FITC-Area at flow rates between 10 and 30 and μL min-1. Events were gated on forward and side scatter and a threshold were set by side-scatter (5000), with doublets discriminated against using standard FSC-Area *vs* FSC-Height and SSC-Area *vs* SSC-Height plots. At least 25 000 events were recorded for cytometry analysis, while directed evolution libraries screened 20 000−80 000 events per sort. For directed evolution screening, cells were sorted directly into LB (with antibiotic), then cultured overnight at 37 °C, shaking at 300 rpm, in culture tubes (Nunc). This culture was then used to inoculate for another day of sorting after being prepared, as above. To obtain the caffeine responsive TFs, the library was toggled between two conditions. First, cells were grown in the presence of 1 mM Caffeine and variants displaying low fluorescence were collected (<5% of the original library). In the subsequent sort, cells were grown in the absence of any ligand and variants that displayed high fluorescence were collected (<10% of the library). Gates were based on percentages of the population rather than FITC values, though they were guided by controls with known cytometry performance—the original K85S (P^S) variant for the repressed state, and the lac stop control for the high GFP state. The low sort was done twice, while the high GFP sort was repeated 6 consecutive times to enrich the desired population and filter out false positives. Following the final sorts, individual colonies were screened *via* the microplate assay to verify phenotype and determine performance characteristics.

Statistical Analysis. Dose response curves were constructed using Graphpad Prism 8.3.1. First, concentrations were transformed into $\log_{10}$ and points were then fit to a log(agonist) *vs* response−variable slope (four parameter) curve using least-squares regression and strict conversion with a maximum of 100 000 iterations. Outliers were detected and eliminated at the Q = 1% level (indicating ≤1% False Discovery Rate) and each replicate Y value was considered as an independent point. Confidence bands are depicted at the 95% confidence interval and depict the likely location of the TRUE curve. Data points represent the mean of 6 biological replicates and error bars represent the standard error of the mean (SEM). Phenotypes were determined by first comparing the mean GFP (fluorescent) output for n = 6 biological replicates in the presence and absence of inducer utilizing a two-tailed Student's t test, allowing for unequal variances. The significance level was set to α = 0.001. For each variant, the dynamic range (or fold antirepression) was calculated by dividing the GFP output in the absence of inducer (the "ON" state) by the GFP output in the presence of the corresponding ligand (the "OFF" or antirepressed state). When probing the specificity of variants toward a variety of ligands, a one-way ANOVA followed by a *post hoc* Dunnett multiple comparison test was performed using the no inducer state as the control. Once again, data points represent the mean of 6 biological replicates and error bars represent the standard error of the mean (SEM).

■ ASSOCIATED CONTENT

Supporting Information

The Supporting Information is available free of charge at https://pubs.acs.org/doi/10.1021/acssynbio.0c00582.

Primary sequence and structural alignments, mutations information, dose response curves, response function parameters, genetic constructs and plasmids information, and tunable NOR operations (PDF)

■ AUTHOR INFORMATION

Corresponding Author

Corey J. Wilson − *Georgia Institute of Technology, School of Chemical & Biomolecular Engineering, Atlanta, Georgia 30332-0100, United States;* orcid.org/0000-0003-3040-1676; Email: corey.wilson@chbe.gatech.edu

Author

Ronald Rondon − *Georgia Institute of Technology, School of Chemical & Biomolecular Engineering, Atlanta, Georgia 30332-0100, United States*

Complete contact information is available at: https://pubs.acs.org/10.1021/acssynbio.0c00582

Author Contributions

R.R. and C.J.W. conceived the study and designed the experiments; R.R. performed experiments; R.R. and C.J.W. analyzed the data; R.R. and C.J.W. wrote the manuscript with input from all the authors.

Notes

The authors declare no competing financial interest.

■ ACKNOWLEDGMENTS

This work was supported by National Science Foundation grants GCR 1934836; MCB 1921061; CBET 1844289; CBET 1804639; and MCB 1747439 all awarded to CJW.

REFERENCES

(1) Cameron, D. E., Bashor, C. J., and Collins, J. J. (2014) A brief history of synthetic biology. *Nat. Rev. Microbiol. 12*, 381−390.

(2) Auslander, S., Auslander, D., and Fussenegger, M. (2017) Synthetic Biology-The Synthesis of Biology. *Angew. Chem., Int. Ed. 56*, 6396−6419.

(3) Carbonell, P., Jervis, A. J., Robinson, C. J., Yan, C., Dunstan, M., Swainston, N., Vinaixa, M., Hollywood, K. A., Currin, A., Rattray, N. J. W., Taylor, S., Spiess, R., Sung, R., Williams, A. R., Fellows, D., Stanford, N. J., Mulherin, P., Le Feuvre, R., Barran, P., Goodacre, R., Turner, N. J., Goble, C., Chen, G. G., Kell, D. B., Micklefield, J., Breitling, R., Takano, E., Faulon, J. L., and Scrutton, N. S. (2018) An automated Design-Build-Test-Learn pipeline for enhanced microbial production of fine chemicals. *Commun. Biol. 1*, 66.

(4) Xie, M., Ye, H., Wang, H., Charpin-El Hamri, G., Lormeau, C., Saxena, P., Stelling, J., and Fussenegger, M. (2016) beta-cell-mimetic designer cells provide closed-loop glycemic control. *Science 354*, 1296−1301.

(5) Bai, P., Ye, H., Xie, M., Saxena, P., Zulewski, H., Charpin-El Hamri, G., Djonov, V., and Fussenegger, M. (2016) A synthetic biology-based device prevents liver injury in mice. *J. Hepatol. 65*, 84−94.

(6) Wang, B., Barahona, M., and Buck, M. (2013) A modular cell-based biosensor using engineered genetic logic circuits to detect and integrate multiple environmental signals. *Biosens. Bioelectron. 40*, 368−376.

(7) de Mora, K., Joshi, N., Balint, B. L., Ward, F. B., Elfick, A., and French, C. E. (2011) A pH-based biosensor for detection of arsenic in drinking water. *Anal. Bioanal. Chem. 400*, 1031−1039.

(8) Stocker, J., Balluch, D., Gsell, M., Harms, H., Feliciano, J., Daunert, S., Malik, K. A., and van der Meer, J. R. (2003) Development of a set of simple bacterial biosensors for quantitative and rapid measurements of arsenite and arsenate in potable water. *Environ. Sci. Technol. 37*, 4743−4750.

(9) Mimee, M., Nadeau, P., Hayward, A., Carim, S., Flanagan, S., Jerger, L., Collins, J., McDonnell, S., Swartwout, R., Citorik, R. J., Bulovic, V., Langer, R., Traverso, G., Chandrakasan, A. P., and Lu, T. K. (2018) An ingestible bacterial-electronic system to monitor gastrointestinal health. *Science 360*, 915−918.

(10) Riglar, D. T., Giessen, T. W., Baym, M., Kerns, S. J., Niederhuber, M. J., Bronson, R. T., Kotula, J. W., Gerber, G. K., Way, J. C., and Silver, P. A. (2017) Engineered bacteria can function in the mammalian gut long-term as live diagnostics of inflammation. *Nat. Biotechnol. 35*, 653−658.

(11) Courbet, A., Endy, D., Renard, E., Molina, F., and Bonnet, J. (2015) Detection of pathological biomarkers in human clinical samples via amplifying genetic switches and logic gates. *Sci. Transl. Med. 7*, 289ra283.

(12) Auslander, S., and Fussenegger, M. (2017) Synthetic RNA-based switches for mammalian gene expression control. *Curr. Opin. Biotechnol. 48*, 54−60.

(13) Auslander, S., and Fussenegger, M. (2013) From gene switches to mammalian designer cells: present and future prospects. *Trends Biotechnol. 31*, 155−168.

(14) Finn, R. D., Attwood, T. K., Babbitt, P. C., Bateman, A., Bork, P., Bridge, A. J., Chang, H. Y., Dosztanyi, Z., El-Gebali, S., Fraser, M., Gough, J., Haft, D., Holliday, G. L., Huang, H., Huang, X., Letunic, I., Lopez, R., Lu, S., Marchler-Bauer, A., Mi, H., Mistry, J., Natale, D. A., Necci, M., Nuka, G., Orengo, C. A., Park, Y., Pesseat, S., Piovesan, D., Potter, S. C., Rawlings, N. D., Redaschi, N., Richardson, L., Rivoire, C., Sangrador-Vegas, A., Sigrist, C., Sillitoe, I., Smithers, B., Squizzato, S., Sutton, G., Thanki, N., Thomas, P. D., Tosatto, S. C., Wu, C. H., Xenarios, I., Yeh, L. S., Young, S. Y., and Mitchell, A. L. (2017) InterPro in 2017-beyond protein family and domain annotations. *Nucleic Acids Res. 45*, D190−D199.

(15) Lin, J. L., Wagner, J. M., and Alper, H. S. (2017) Enabling tools for high-throughput detection of metabolites: Metabolic engineering and directed evolution applications. *Biotechnol. Adv. 35*, 950−970.

(16) Werten, S., Schneider, J., Palm, G. J., and Hinrichs, W. (2016) Modular organisation of inducer recognition and allostery in the tetracycline repressor. *FEBS J. 283*, 2102−2114.

(17) Chan, C. T., Lee, J. W., Cameron, D. E., Bashor, C. J., and Collins, J. J. (2016) 'Deadman' and 'Passcode' microbial kill switches for bacterial containment. *Nat. Chem. Biol. 12*, 82−86.

(18) Rondon, R. E., Groseclose, T. M., Short, A. E., and Wilson, C. J. (2019) Transcriptional programming using engineered systems of transcription factors and genetic architectures. *Nat. Commun. 10*, 4784.

(19) Dimas, R. P., Jordan, B. R., Jiang, X. L., Martini, C., Glavy, J. S., Patterson, D. P., Morcos, F., and Chan, C. T. Y. (2019) Engineering DNA recognition and allosteric response properties of TetR family proteins by using a module-swapping strategy. *Nucleic Acids Res. 47*, 8913−8925.

(20) Rondon, R. E., and Wilson, C. J. (2019) Engineering a New Class of Anti-LacI Transcription Factors with Alternate DNA Recognition. *ACS Synth. Biol. 8*, 307−317.

(21) De Paepe, B., Maertens, J., Vanholme, B., and De Mey, M. (2019) Chimeric LysR-Type Transcriptional Biosensors for Customizing Ligand Specificity Profiles toward Flavonoids. *ACS Synth. Biol. 8*, 318−331.

(22) Juarez, J. F., Lecube-Azpeitia, B., Brown, S. L., Johnston, C. D., and Church, G. M. (2018) Biosensor libraries harness large classes of binding domains for construction of allosteric transcriptional regulators. *Nat. Commun. 9*, 3101.

(23) Shis, D. L., Hussain, F., Meinhardt, S., Swint-Kruse, L., and Bennett, M. R. (2014) Modular, multi-input transcriptional logic gating with orthogonal LacI/GalR family chimeras. *ACS Synth. Biol. 3*, 645−651.

(24) Snoek, T., Chaberski, E. K., Ambri, F., Kol, S., Bjorn, S. P., Pang, B., Barajas, J. F., Welner, D. H., Jensen, M. K., and Keasling, J. D. (2020) Evolution-guided engineering of small-molecule biosensors. *Nucleic Acids Res. 48*, e3.

(25) Ellefson, J. W., Ledbetter, M. P., and Ellington, A. D. (2018) Directed evolution of a synthetic phylogeny of programmable Trp repressors. *Nat. Chem. Biol. 14*, 361−367.

(26) Tang, S. Y., Fazelinia, H., and Cirino, P. C. (2008) AraC regulatory protein mutants with altered effector specificity. *J. Am. Chem. Soc. 130*, 5267−5271.

(27) Collins, C. H., Leadbetter, J. R., and Arnold, F. H. (2006) Dual selection enhances the signaling specificity of a variant of the quorum-sensing transcriptional activator LuxR. *Nat. Biotechnol. 24*, 708−712.

(28) Meyer, A. J., Segall-Shapiro, T. H., Glassey, E., Zhang, J., and Voigt, C. A. (2019) Escherichia coli "Marionette" strains with 12 highly optimized small-molecule sensors. *Nat. Chem. Biol. 15*, 196−204.

(29) Richards, D. H., Meyer, S., and Wilson, C. J. (2017) Fourteen Ways to Reroute Cooperative Communication in the Lactose Repressor: Engineering Regulatory Proteins with Alternate Repressive Functions. *ACS Synth. Biol. 6*, 6−12.

(30) Poelwijk, F. J., de Vos, M. G., and Tans, S. J. (2011) Tradeoffs and optimality in the evolution of gene regulation. *Cell 146*, 462−470.

(31) Groseclose, T. M., Rondon, R. E., Herde, Z. D., Aldrete, C. A., and Wilson, C. J. (2020) Engineered systems of inducible anti-repressors for the next generation of biological programming. *Nat. Commun. 11*, 4440.

(32) Choi, K. Y., Lu, F., and Zalkin, H. (1994) Mutagenesis of amino acid residues required for binding of corepressors to the purine repressor. *J. Biol. Chem. 269*, 24066−24072.

(33) He, B., Choi, K. Y., and Zalkin, H. (1993) Regulation of Escherichia coli glnB, prsA, and speA by the purine repressor. *J. Bacteriol. 175*, 3598−3606.

(34) Wilson, H. R., and Turnbough, C. L., Jr. (1990) Role of the purine repressor in the regulation of pyrimidine gene expression in Escherichia coli K-12. *J. Bacteriol. 172*, 3208−3213.

(35) Choi, K. Y., and Zalkin, H. (1990) Regulation of Escherichia coli pyrC by the purine regulon repressor protein. *J. Bacteriol. 172*, 3201−3207.

https://dx.doi.org/10.1021/acssynbio.0c00582
ACS Synth. Biol. 2021, 10, 552−565

(36) Meng, L. M., Kilstrup, M., and Nygaard, P. (1990) Autoregulation of PurR repressor synthesis and involvement of purR in the regulation of purB, purC, purL, purMN and guaBA expression in Escherichia coli. *Eur. J. Biochem. 187*, 373−379.
(37) Kilstrup, M., Meng, L. M., Neuhard, J., and Nygaard, P. (1989) Genetic evidence for a repressor of synthesis of cytosine deaminase and purine biosynthesis enzymes in Escherichia coli. *J. Bacteriol. 171*, 2124−2127.
(38) Swint-Kruse, L., Elam, C. R., Lin, J. W., Wycuff, D. R., and Shive Matthews, K. (2001) Plasticity of quaternary structure: twenty-two ways to form a LacI dimer. *Protein Sci. 10*, 262−276.
(39) Schumacher, M. A., Choi, K. Y., Lu, F., Zalkin, H., and Brennan, R. G. (1995) Mechanism of corepressor-mediated specific DNA binding by the purine repressor. *Cell 83*, 147−155.
(40) Friedman, A. M., Fischmann, T. O., and Steitz, T. A. (1995) Crystal structure of lac repressor core tetramer and its implications for DNA looping. *Science 268*, 1721−1727.
(41) Schumacher, M. A., Choi, K. Y., Zalkin, H., and Brennan, R. G. (1994) Crystal structure of LacI member, PurR, bound to DNA: minor groove binding by alpha helices. *Science 266*, 763−770.
(42) Wang, Y., Deng, M., Deng, B., Ye, L., Fei, X., and Huang, Z. (2019) Study on the diagnosis of gout with xanthine and hypoxanthine. *J. Clin. Lab. Anal. 33*, e22868.
(43) Farthing, D. E., Farthing, C. A., and Xi, L. (2015) Inosine and hypoxanthine as novel biomarkers for cardiac ischemia: from bench to point-of-care. *Exp. Biol. Med. (London, U. K.) 240*, 821−831.
(44) Turgan, N., Habif, S., Gulter, C., Senol, B., Mutaf, I., Ozmen, D., Bayindir, O., Boydak, B., and Turgan, N. (1999) Urinary hypoxanthine and xanthine levels in acute coronary syndromes. *Int. J. Clin. Lab. Res. 29*, 162−165.
(45) Singh, N., Shreshtha, A. K., Thakur, M. S., and Patra, S. (2018) Xanthine scaffold: scope and potential in drug development. *Heliyon 4*, e00829.
(46) Fritea, L., Tertis, M., Sandulescu, R., and Cristea, C. (2018) Enzyme-Graphene Platforms for Electrochemical Biosensor Design With Biomedical Applications. *Methods Enzymol. 609*, 293−333.
(47) Chang, Y. L., Hsu, Y. J., Chen, Y., Wang, Y. W., and Huang, S. M. (2017) Theophylline exhibits anti-cancer activity via suppressing SRSF3 in cervical and breast cancer cell lines. *Oncotarget 8*, 101461−101474.
(48) Martinez-Pinilla, E., Onatibia-Astibia, A., and Franco, R. (2015) The relevance of theobromine for the beneficial effects of cocoa consumption. *Front. Pharmacol. 6*, 30.
(49) Dubuis, E., Wortley, M. A., Grace, M. S., Maher, S. A., Adcock, J. J., Birrell, M. A., and Belvisi, M. G. (2014) Theophylline inhibits the cough reflex through a novel mechanism of action. *J. Allergy Clin. Immunol. 133*, 1588−1598.
(50) Monteiro, J. P., Alves, M. G., Oliveira, P. F., and Silva, B. M. (2016) Structure-Bioactivity Relationships of Methylxanthines: Trying to Make Sense of All the Promises and the Drawbacks. *Molecules*, DOI: 10.3390/molecules21080974.
(51) Wikoff, D., Welsh, B. T., Henderson, R., Brorby, G. P., Britt, J., Myers, E., Goldberger, J., Lieberman, H. R., O'Brien, C., Peck, J., Tenenbein, M., Weaver, C., Harvey, S., Urban, J., and Doepker, C. (2017) Systematic review of the potential adverse effects of caffeine consumption in healthy adults, pregnant women, adolescents, and children. *Food Chem. Toxicol. 109*, 585−648.
(52) Bojar, D., Scheller, L., Hamri, G. C., Xie, M., and Fussenegger, M. (2018) Caffeine-inducible gene switches controlling experimental diabetes. *Nat. Commun. 9*, 2318.
(53) Michener, J. K., and Smolke, C. D. (2012) High-throughput enzyme evolution in Saccharomyces cerevisiae using a synthetic RNA switch. *Metab. Eng. 14*, 306−316.
(54) Gutierrez, A. E., Shah, P., Rex, A. E., Nguyen, T. C., Kenkare, S. P., Barrick, J. E., and Mishler, D. M. (2019) Bioassay for Determining the Concentrations of Caffeine and Individual Methylxanthines in Complex Samples. *Appl. Environ. Microbiol.*, DOI: 10.1128/AEM.01965-19.
(55) Quandt, E. M., Hammerling, M. J., Summers, R. M., Otoupal, P. B., Slater, B., Alnahhas, R. N., Dasgupta, A., Bachman, J. L., Subramanian, M. V., and Barrick, J. E. (2013) Decaffeination and measurement of caffeine content by addicted Escherichia coli with a refactored N-demethylation operon from Pseudomonas putida CBB5. *ACS Synth. Biol. 2*, 301−307.
(56) Dash, S. S., and Gummadi, S. N. (2008) Inducible nature of the enzymes involved in catabolism of caffeine and related methylxanthines. *J. Basic Microbiol. 48*, 227−233.
(57) Mazumder, M., and McMillen, D. R. (2014) Design and characterization of a dual-mode promoter with activation and repression capability for tuning gene expression in yeast. *Nucleic Acids Res. 42*, 9514−9522.
(58) Cronin, C. A., Gluba, W., and Scrable, H. (2001) The lac operator-repressor system is functional in the mouse. *Genes Dev. 15*, 1506−1517.
(59) Ulmasov, B., Capone, J., and Folk, W. (1997) Regulated expression of plant tRNA genes by the prokaryotic tet and lac repressors. *Plant Mol. Biol. 35*, 417−424.
(60) Hu, M. C., and Davidson, N. (1987) The inducible lac operator-repressor system is functional in mammalian cells. *Cell 48*, 555−566.
(61) Tungtur, S., Meinhardt, S., and Swint-Kruse, L. (2010) Comparing the functional roles of nonconserved sequence positions in homologous transcription repressors: implications for sequence/function analyses. *J. Mol. Biol. 395*, 785−802.
(62) Wu, J., Jiang, P., Chen, W., Xiong, D., Huang, L., Jia, J., Chen, Y., Jin, J. M., and Tang, S. Y. (2017) Design and application of a lactulose biosensor. *Sci. Rep. 7*, 45994.
(63) Taylor, N. D., Garruss, A. S., Moretti, R., Chan, S., Arbing, M. A., Cascio, D., Rogers, J. K., Isaacs, F. J., Kosuri, S., Baker, D., Fields, S., Church, G. M., and Raman, S. (2016) Engineering an allosteric transcription factor to respond to new ligands. *Nat. Methods 13*, 177−183.
(64) Galvao, T. C., Mencia, M., and de Lorenzo, V. (2007) Emergence of novel functions in transcriptional regulators by regression to stem protein types. *Mol. Microbiol. 65*, 907−919.
(65) Gander, M. W., Vrana, J. D., Voje, W. E., Carothers, J. M., and Klavins, E. (2017) Digital logic circuits in yeast with CRISPR-dCas9 NOR gates. *Nat. Commun. 8*, 15459.
(66) Milk, L., Daber, R., and Lewis, M. (2010) Functional rules for lac repressor-operator associations and implications for protein-DNA interactions. *Protein Sci. 19*, 1162−1172.
(67) Herde, Z. D., Short, A. E., Kay, V. E., Huang, B. D., Realff, M. J., and Wilson, C. J. (2020) Engineering allosteric communication. *Curr. Opin. Struct. Biol. 63*, 115−122.
(68) Meyer, S., Ramot, R., Kishore Inampudi, K., Luo, B., Lin, C., Amere, S., and Wilson, C. J. (2013) Engineering alternate cooperative-communications in the lactose repressor protein scaffold. *Protein Eng., Des. Sel. 26*, 433−443.
(69) Zhan, H., Camargo, M., and Matthews, K. S. (2010) Positions 94−98 of the lactose repressor N-subdomain monomer-monomer interface are critical for allosteric communication. *Biochemistry 49*, 8636−8645.
(70) Swint-Kruse, L., Zhan, H., and Matthews, K. S. (2005) Integrated insights from simulation, experiment, and mutational analysis yield new details of LacI function. *Biochemistry 44*, 11201−11213.
(71) Meinhardt, S., Manley, M. W., Jr., Parente, D. J., and Swint-Kruse, L. (2013) Rheostats and toggle switches for modulating protein function. *PLoS One 8*, e83502.
(72) Gorochowski, T. E., van den Berg, E., Kerkman, R., Roubos, J. A., and Bovenberg, R. A. (2014) Using synthetic biological parts and microbioreactors to explore the protein expression characteristics of Escherichia coli. *ACS Synth. Biol. 3*, 129−139.
(73) Moser, F., Broers, N. J., Hartmans, S., Tamsir, A., Kerkman, R., Roubos, J. A., Bovenberg, R., and Voigt, C. A. (2012) Genetic circuit performance under conditions relevant for industrial bioreactors. *ACS Synth. Biol. 1*, 555−564.

(74) Cardinale, S., and Arkin, A. P. (2012) Contextualizing context for synthetic biology–identifying causes of failure of synthetic biological systems. *Biotechnol. J. 7*, 856−866.
(75) Gorochowski, T. E., Chelysheva, I., Eriksen, M., Nair, P., Pedersen, S., and Ignatova, Z. (2019) Absolute quantification of translational regulation and burden using combined sequencing approaches. *Mol. Syst. Biol. 15*, e8719.
(76) Qian, Y., Huang, H. H., Jimenez, J. I., and Del Vecchio, D. (2017) Resource Competition Shapes the Response of Genetic Circuits. *ACS Synth. Biol. 6*, 1263−1272.
(77) Gorochowski, T. E., Avcilar-Kucukgoze, I., Bovenberg, R. A., Roubos, J. A., and Ignatova, Z. (2016) A Minimal Model of Ribosome Allocation Dynamics Captures Trade-offs in Expression between Endogenous and Synthetic Genes. *ACS Synth. Biol. 5*, 710−720.
(78) Gyorgy, A., Jimenez, J. I., Yazbek, J., Huang, H. H., Chung, H., Weiss, R., and Del Vecchio, D. (2015) Isocost Lines Describe the Cellular Economy of Genetic Circuits. *Biophys. J. 109*, 639−646.
(79) Nielsen, A. A., Der, B. S., Shin, J., Vaidyanathan, P., Paralanov, V., Strychalski, E. A., Ross, D., Densmore, D., and Voigt, C. A. (2016) Genetic circuit design automation. *Science 352*, aac7341.
(80) Brophy, J. A., and Voigt, C. A. (2014) Principles of genetic circuit design. *Nat. Methods 11*, 508−520.
(81) Thompson, M. G., Pearson, A. N., Barajas, J. F., Cruz-Morales, P., Sedaghatian, N., Costello, Z., Garber, M. E., Incha, M. R., Valencia, L. E., Baidoo, E. E. K., Martin, H. G., Mukhopadhyay, A., and Keasling, J. D. (2020) Identification, Characterization, and Application of a Highly Sensitive Lactam Biosensor from Pseudomonas putida. *ACS Synth. Biol. 9*, 53−62.
(82) Koch, M., Pandi, A., Borkowski, O., Batista, A. C., and Faulon, J. L. (2019) Custom-made transcriptional biosensors for metabolic engineering. *Curr. Opin. Biotechnol. 59*, 78−84.
(83) Zhang, F., Carothers, J. M., and Keasling, J. D. (2012) Design of a dynamic sensor-regulator system for production of chemicals and fuels derived from fatty acids. *Nat. Biotechnol. 30*, 354−359.
(84) Kim, H. J., Jeong, H., and Lee, S. J. (2018) Synthetic biology for microbial heavy metal biosensors. *Anal. Bioanal. Chem. 410*, 1191−1203.
(85) van der Meer, J. R., and Belkin, S. (2010) Where microbiology meets microengineering: design and applications of reporter bacteria. *Nat. Rev. Microbiol. 8*, 511−522.
(86) Machado, L. F. M., Currin, A., and Dixon, N. (2019) Directed evolution of the PcaV allosteric transcription factor to generate a biosensor for aromatic aldehydes. *J. Biol. Eng. 13*, 91.
(87) Galvao, T. C., and de Lorenzo, V. (2006) Transcriptional regulators a la carte: engineering new effector specificities in bacterial regulatory proteins. *Curr. Opin. Biotechnol. 17*, 34−42.
(88) Ashihara, H., and Crozier, A. (2001) Caffeine: a well known but little mentioned compound in plant science. *Trends Plant Sci. 6*, 407−413.
(89) Barone, J. J., and Roberts, H. R. (1996) Caffeine consumption. *Food Chem. Toxicol. 34*, 119−129.
(90) Mohanty, S. K., Yu, C. L., Gopishetty, S., and Subramanian, M. (2014) Validation of caffeine dehydrogenase from Pseudomonas sp. strain CBB1 as a suitable enzyme for a rapid caffeine detection and potential diagnostic test. *J. Agric. Food Chem. 62*, 7939−7946.
(91) Jain, S., Srivastava, A. S., Verma, R. P., and Maggu, G. (2019) Caffeine addiction: Need for awareness and research and regulatory measures. *Asian J. Psychiatr 41*, 73−75.
(92) Temple, J. L., Bernard, C., Lipshultz, S. E., Czachor, J. D., Westphal, J. A., and Mestre, M. A. (2017) The Safety of Ingested Caffeine: A Comprehensive Review. *Front. Psychiatry 8*, 80.
(93) Buerge, I. J., Poiger, T., Muller, M. D., and Buser, H. R. (2006) Combined sewer overflows to surface waters detected by the anthropogenic marker caffeine. *Environ. Sci. Technol. 40*, 4096−4102.
(94) Buerge, I. I., Poiger, T., Muller, M. D., and Buser, H. R. (2003) Caffeine, an anthropogenic marker for wastewater comtamination of surface waters. *Environ. Sci. Technol. 37*, 691−700.
(95) Horrigan, L. A., Kelly, J. P., and Connor, T. J. (2006) Immunomodulatory effects of caffeine: friend or foe? *Pharmacol. Ther. 111*, 877−892.
(96) Simons, F. E., Becker, A. B., Simons, K. J., and Gillespie, C. A. (1985) The bronchodilator effect and pharmacokinetics of theobromine in young patients with asthma. *J. Allergy Clin. Immunol. 76*, 703−707.
(97) Luria, S. E., Adams, J. N., and Ting, R. C. (1960) Transduction of lactose-utilizing ability among strains of E. coli and S. dysenteriae and the properties of the transducing phage particles. *Virology 12*, 348−390.
(98) Pettersen, E. F., Goddard, T. D., Huang, C. C., Couch, G. S., Greenblatt, D. M., Meng, E. C., and Ferrin, T. E. (2004) UCSF Chimera–a visualization system for exploratory research and analysis. *J. Comput. Chem. 25*, 1605−1612.

https://dx.doi.org/10.1021/acssynbio.0c00582
ACS Synth. Biol. 2021, 10, 552−565